

Gamma-ray spectroscopy of $^{60,61}\text{Zn}$ and $^{59,60}\text{Cu}$

R. B. Schubank,* J. A. Cameron, and V. P. Janzen†

Tandem Accelerator Laboratory, McMaster University, Hamilton, Ontario, Canada L8S 4K1

(Received 10 April 1989)

The levels of $^{60,61}\text{Zn}$ and $^{59,60}\text{Cu}$ have been investigated using γ - γ coincidence spectroscopy in the reactions $^{58}\text{Ni}(\alpha, n)^{61}\text{Zn}$ at 13 MeV, $^{58}\text{Ni}(\alpha, n\gamma)^{61}\text{Zn}$ at 11.5, 15, and 20 MeV, $^{58}\text{Ni}({}^6\text{Li}, p2n\gamma)^{61}\text{Zn}$ at 30 MeV, $^{54}\text{Fe}({}^{10}\text{B}, p2n\gamma)^{61}\text{Zn}$ at 45 MeV, $^{40}\text{Ca}({}^{24}\text{Mg}, 2pn\gamma)^{61}\text{Zn}$ at 65 and 80 MeV, $^{58}\text{Ni}({}^3\text{He}, n\gamma)^{60}\text{Zn}$ at 8 and 12 MeV, $^{40}\text{Ca}({}^{23}\text{Na}, p2n\gamma)^{60}\text{Zn}$ at 70 MeV, $^{58}\text{Ni}({}^3\text{He}, pn\gamma)^{59}\text{Cu}$ at 12 MeV, $^{58}\text{Ni}(\alpha, pn\gamma)^{60}\text{Cu}$ at 20 MeV, and $^{40}\text{Ca}({}^{23}\text{Na}, 2pn\gamma)^{60}\text{Cu}$ at 70 MeV. In the helium-induced reactions, spectra were gated with neutron coincidences. New levels have been found in all the nuclides studied, and a number of new spin assignments were made on the basis of n - γ angular correlations. The results are compared with earlier γ -ray and particle studies, and with preexisting shell-model predictions.

I. INTRODUCTION

The light Cu and Zn nuclei lie just beyond the closure of the $f_{7/2}$ shell at ^{56}Ni , with both protons and neutrons occupying the $p_{3/2}$, $f_{5/2}$, and $p_{1/2}$ subshells. Shell-model calculations of such nuclei are based either on reaction matrix elements or empirically determined interactions. Examples of the former type^{1,2} provide spectra and properties of Cu and Zn nuclei with $A \leq 60$, while Refs. 3 and 4 deal with all the isotopes. Other attempts to model such nuclei have used weak coupling between a valence particle or cluster and a vibrating core.^{5,6} Such calculations have not dealt with the light isotopes explored here. An additional aspect of the nuclei in this mass region is the presence of the $g_{9/2}$ subshell. Having opposite parity, single-particle excitations to the $g_{9/2}$ shell are not mixed with the states arising from the f and p shells. However, as the number of particles beyond ^{56}Ni increases, the energy of the $\frac{9}{2}^+$ excitation decreases smoothly.

The experimental situation in the light Zn isotopes is made difficult by the lack of targets for single-particle transfer and the propensity of $Z \approx N$ compound nuclei for charged particle decay. In spite of these difficulties, there have been a number of heavy-ion transfer and gamma-ray studies of ^{60}Zn (Refs. 7–14) and ^{61}Zn (Refs. 11 and 15–17). It was the object of this study to confirm and extend the γ -ray work, to aid a fuller comparison with the calculations. The experiments included $({}^3, {}^4\text{He}, n)$ reactions on ^{58}Ni , using neutron and gamma detection, singly and in coincidence, and angular distributions, as well as γ - γ coincidence spectroscopy with a number of heavy-ion-induced reactions on ^{58}Ni , ^{54}Fe , and ^{40}Ca . As a by-product, information was obtained for the more abundantly produced nuclei $^{59,60}\text{Cu}$. Much γ -ray work has already appeared for these nuclides,^{7,18–25} but a number of new results have been obtained and are reported here.

II. EXPERIMENTAL

The experiments were carried out at the McMaster FN Tandem accelerator using ${}^3, {}^4\text{He}$, ${}^6\text{Li}$, and ${}^{23}\text{Na}$ beams from a charge exchange source and other heavy ions

from a sputter source. Self-supporting metal targets were used in small stainless steel or plastic target chambers using tantalum collimators and ${}^{208}\text{Pb}$ or gold beam stops. Target thicknesses were about $50 \mu\text{g}/\text{cm}^2$ for neutron spectroscopy and heavy-ion experiments and over $1 \text{ mg}/\text{cm}^2$ for the helium-induced γ , γ - γ , n - γ , and angular distribution measurements.

Neutron spectra were observed using a Seforad ${}^3\text{He}$ -filled detector²⁶ and γ rays in an array of assorted Ge and Ge(Li) detectors. For the n - γ experiments, a $5 \times 5 \text{ cm}$ plastic scintillator with standard pulse-shape discrimination was used, at 0° behind 3 cm of lead, with two Ge detectors at 90° to the beam and to each other. For the heavy-ion γ - γ experiments, an array of 5 Ge detectors was gated by a multiplicity filter of 6 NaI counters. Data were recorded in event mode on tape. The Ge detectors were calibrated in energy and efficiency using an assortment of standard γ sources, and beam-induced γ radioactivity. The neutron detector calibration was made using the ${}^{27}\text{Al}(p, n){}^{27}\text{Si}$ reaction [$Q = -5.594(1) \text{ MeV}$] at a number of incident energies.

In addition to energy information in the n - γ and γ - γ experiments, timing was also recorded so that any nanosecond isomers could be found. For the major γ transitions, where good statistical precision was obtained, centroid shifts down to about 1 ns were in principle discernable. In the angular distributions, Doppler shifts as small as 0.2 keV could be observed by taking advantage of the internal calibrations provided by beam-induced target radioactivity. In the helium reactions, maximum shifts were 0.4% so Doppler shift attenuation method (DSAM) lifetimes up to about 1 ps were measurable.

For ^{61}Zn , the principal reaction employed was $^{58}\text{Ni}(\alpha, n\gamma)^{61}\text{Zn}$ at beam energies of 11.5, 15, and 20 MeV. Singles γ , n - γ , γ - γ , and n - γ - γ coincidence spectra were observed. Angular distributions of γ rays in coincidence with neutrons detected at 0° were used to obtain spins and parities of excited states. The detection of the reaction neutron on the beam axis increases the alignment, and consequently the magnitudes of angular distribution coefficients, only slightly compared with those obtained in singles angular distributions. Corrections to the

alignments for top and side feeding were made in a self-consistent manner once a level scheme was established. The mixing ratio phase convention used was that of Rose and Brink²⁷ and the uncertainties were determined using the method of James *et al.*²⁸ The $^{58}\text{Ni}(\alpha, n)^{61}\text{Zn}$ neutron spectrum was measured at a beam energy of 13 MeV. Similar measurements of γ singles, $n\text{-}\gamma$ and $n\text{-}\gamma\text{-}\gamma$ coincidences, and $n\text{-}\gamma$ angular distributions were made for the $^{58}\text{Ni}(^3\text{He}, n\gamma)^{60}\text{Zn}$ reaction at 8 and 12 MeV.

Several heavy-ion fusion-evaporation reactions were attempted. For ^{61}Zn , the most useful were $^{58}\text{Ni}(^6\text{Li}, p2n)$ and $^{54}\text{Fe}(^{10}\text{B}, p2n)$ at 30 and 45 MeV, respectively and $^{40}\text{Ca}(^{24}\text{Mg}, 2pn)$ at 65 and 85 MeV. For ^{60}Zn , only $^{40}\text{Ca}(^{23}\text{Na}, p2n)$ at 70 MeV showed any appreciable strength and no further spectroscopic information was obtained, in spite of the much greater angular momentum involved.

In the higher-energy $^{58}\text{Ni} + ^3,^4\text{He}$ reactions, the yield of the pn exit channel leading to $^{59,60}\text{Cu}$ was high. Analysis of these events, together with those from the $^{40}\text{Ca}(^{23}\text{Na}, 2pn)^{60}\text{Cu}$ reaction led to new levels and transitions for these isotopes.

III. RESULTS

In the reactions studied here, several isotopes of Cu and Zn were found. Although traces of ^{59}Zn were sought carefully both in beam and with beam pulsing, no clear evidence was found. On the other hand, ^{61}Cu was to be seen in abundance, but since its spectroscopy has been extensively reported,¹¹ it is not included here. New results obtained for $^{60,61}\text{Zn}$ and $^{59,60}\text{Cu}$ are given in the following.

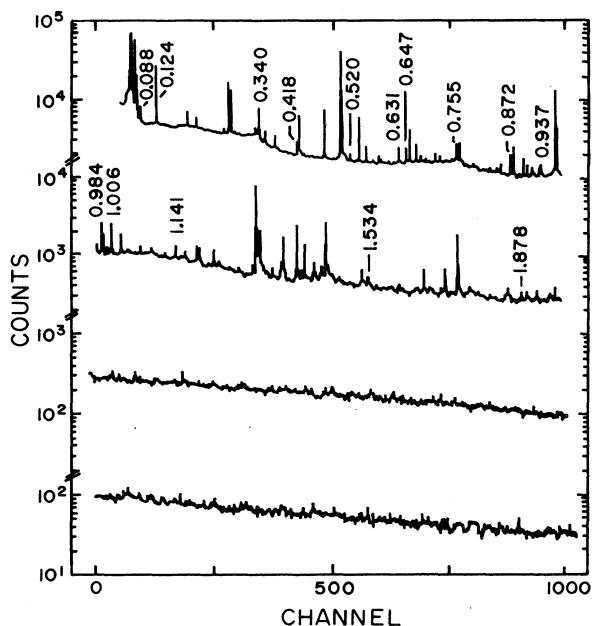


FIG. 1. Singles 4096-channel γ spectrum from $^{58}\text{Ni} + \alpha$ at 15 MeV. Only the ^{61}Zn lines are marked with their energies in MeV. The remainder come from competing reactions, principally $^{58}\text{Ni}(\alpha, p)^{61}\text{Cu}$.

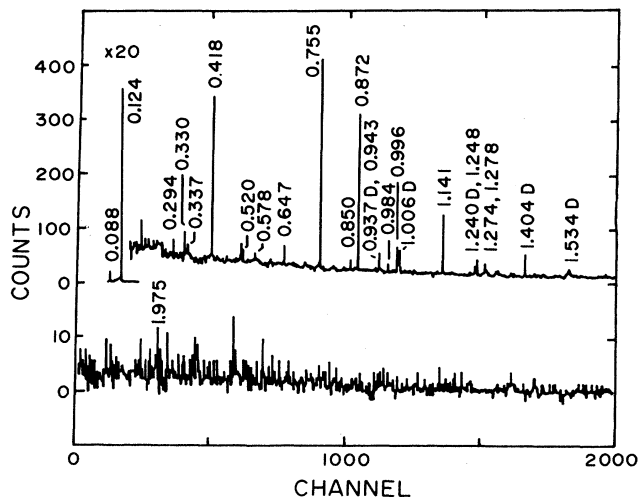


FIG. 2. $^{58}\text{Ni}(\alpha, n\gamma)^{61}\text{Zn}$ neutron-gated spectrum at $E_\alpha = 15$ MeV. (D = doublet, see the text).

A. ^{61}Zn

The singles γ -ray spectrum of $^{58}\text{Ni} + \alpha$ (Fig. 1) is dominated by the $(\alpha, p\gamma)$ reaction to levels in ^{61}Cu , already thoroughly investigated.¹⁵ Only the strongest lines of ^{61}Zn are clearly visible. The value of accepting the low

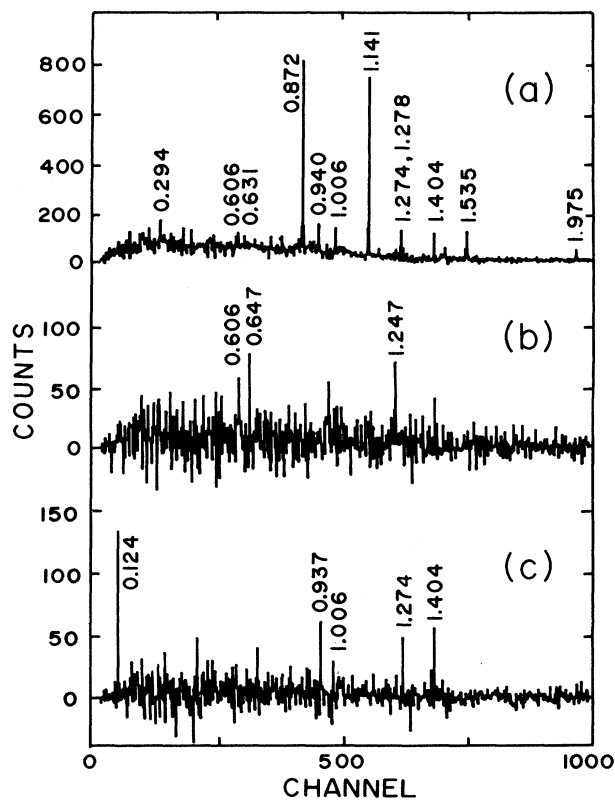


FIG. 3. $^{58}\text{Ni}(\alpha, n\gamma\gamma)^{61}\text{Zn}$ neutron-gated coincidences at $E_\alpha = 15$ MeV. Gates: (a) 0.124 MeV, (b) 0.755 MeV, and (c) 0.872 MeV.

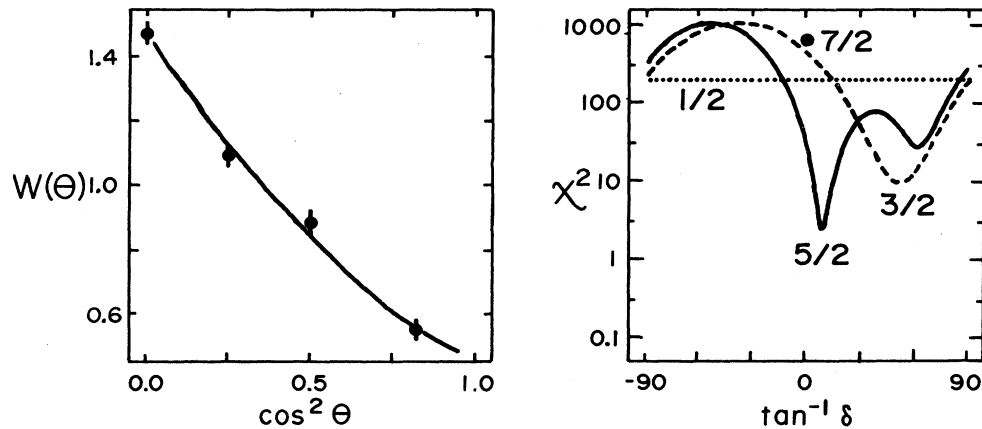


FIG. 4. $^{58}\text{Ni}(\alpha, n\gamma)^{61}\text{Zn}$ neutron-gated angular distribution at $E_\alpha = 15$ MeV, $E_\gamma = 0.755$ MeV. The χ^2 vs $\tan^{-1} \delta$ plot is for the indicated J_i values, for $J_i \rightarrow \frac{3}{2}$.

efficiency of neutron coincidence spectroscopy in observing the $(\alpha, n\gamma)$ channel has been demonstrated in Refs. 16 and 17. The $n\text{-}\gamma$ coincidence spectrum of Fig. 2, taken at $E_\alpha = 15$ MeV, illustrates the selectivity of the neutron detector in this work. Figure 3 shows the quality of the $\gamma\text{-}\gamma$ coincidences obtained for ^{61}Zn .

Figure 4 is an example of the $n\text{-}\gamma$ angular correlation results and the nature of the fitting procedure. The curves of χ^2 vs $\tan^{-1} \delta$, shown for three choices of $J_i \rightarrow \frac{3}{2}$ for the $0.755 \rightarrow 0$ MeV transition, are fairly insensitive to reasonable variations in initial-state population parameters. The absence of observably delayed coincidences places the lifetimes of all the ^{61}Zn levels found below 1 ns. On the other hand, no Doppler shifts were found so it may be inferred that the lifetimes are greater than 1 ps. Although not definitive, these limits allow some restriction in spin-parity assignments using the recommended upper limits of Endt.²⁹

Figure 5 contains a neutron spectrum taken with the ^3He -filled detector at a beam energy of 13 MeV. The peak at low energy is caused by slow neutrons, while the broad high-energy peak is from the (α, n) reaction on ^{12}C .

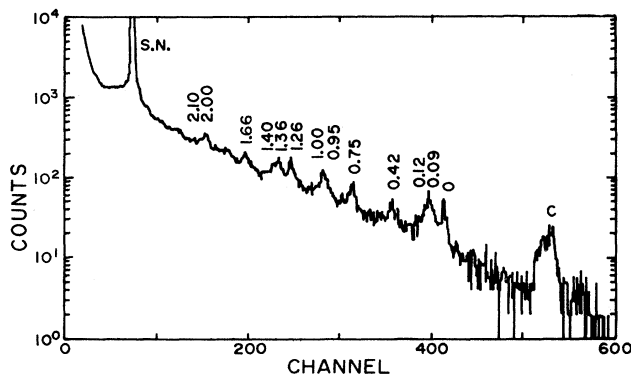


FIG. 5. $^{58}\text{Ni}(\alpha, n)^{61}\text{Zn}$ neutron spectrum at $E_\alpha = 13$ MeV.

From such spectra, a mass excess of $-56.369(8)$ MeV was derived. Table I contains a listing of the energy levels and transitions deduced from the neutron singles, $n\text{-}\gamma$ and $\gamma\text{-}\gamma$ coincidence and $n\text{-}\gamma$ angular distribution measurements. Close doublets occur in ^{61}Zn at 0.938, 1.006, and 1.403 MeV. The relative intensities of these were derived from shifts of the centroids between the $n\text{-}\gamma$ and $n\text{-}\gamma\text{-}\gamma$ spectra. Accordingly, less confidence can be placed on these intensities and angular distributions than on those for clearly resolved lines. Figure 6 is the level scheme of ^{61}Zn based on the preceding work. The top transition was observed only in the heavy-ion reactions. The filled circles indicate observed $\gamma\text{-}\gamma$ coincidence relations.

B. ^{60}Zn

The $n\text{-}\gamma$ spectrum of ^{60}Zn , taken at a ^3He beam energy of 12 MeV, is shown in Fig. 7. Figure 8 is an example of

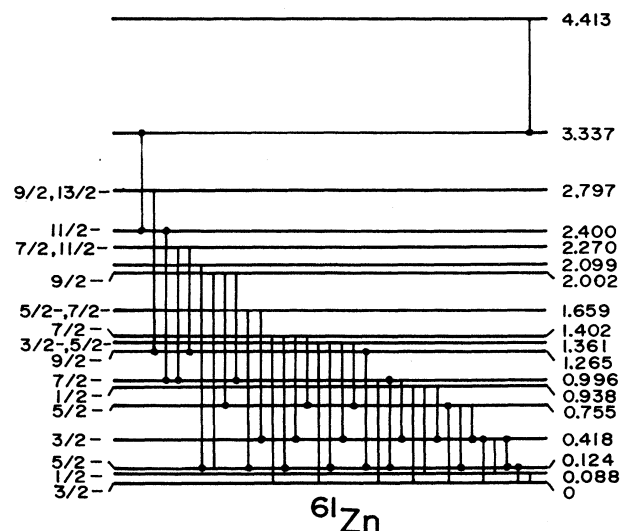


FIG. 6. Proposed level scheme for ^{61}Zn .

the $n\text{-}\gamma\text{-}\gamma$ coincidence spectra at 12 MeV. Table II contains the γ energies and angular distribution coefficients, together with deduced energy levels, decay branching, and spins. As in the ^{61}Zn case, no measurable lifetime effects were found either in coincidence delay or Doppler shift so only broad limits 1 ps to 1 ns can be assigned for the lifetimes of all the levels reported in Fig. 9.

C. ^{59}Cu

In the $^{58}\text{Ni}+^3\text{He}$ experiment intended to further knowledge of ^{60}Zn , many lines of ^{59}Cu were seen, particu-

larly at 12 MeV. By setting gates on the well-known lower transitions,¹⁸ it was possible to observe a few higher transitions, annotated in Table III and shown in Fig. 10. The spin-parity values are from Refs. 18 and 20.

D. ^{60}Cu

At 20 MeV, the $^{58}\text{Ni}+\alpha$ spectrum contains the stronger lines of ^{60}Cu from the np exit channel. The $^{58}\text{Ni}(^3\text{He},p\gamma)^{60}\text{Cu}$ yield is much higher, so coincidences could be found in the $\gamma\text{-}\gamma$ spectra by removing the neutron coincidence requirement. Further transitions were

TABLE I. Levels and transitions in ^{61}Zn .

E_i	E_γ (MeV)	E_f	Branching ratio (%)	A_2	A_4	J_i^π	J_f^π	δ
0.088	0.088	0.000	100	-0.07(6)	-0.04(8)	$\frac{1}{2}^-$	$\frac{3}{2}^-$	
0.124	0.124	0.000	100	-0.13(1)	-0.02(1)	$\frac{5}{2}^-$	$\frac{3}{2}^-$	0.05(2)
0.418	0.418	0.000	85	0.15(4)	0.00(5)	$\frac{3}{2}^-$	$\frac{3}{2}^-$	0.10(5)
	0.330	0.088	10	0.02(10)	0.12(20)		$\frac{1}{2}^-$	-0.27(13)
	0.294	0.124	5	0.26(19)	0.20(26)		$\frac{5}{2}^-$	0.44(37)
0.755	0.755	0.000	97	-0.66(2)	0.10(2)	$\frac{5}{2}^-$	$\frac{3}{2}^-$	0.07(4)
	0.631	0.124	2				$\frac{5}{2}^-$	
	0.337	0.418	1				$\frac{3}{2}^-$	
0.938	0.938	0.000	38				$\frac{3}{2}^-$	
	0.850	0.088	36				$\frac{1}{2}^-$	
	0.520	0.418	26				$\frac{3}{2}^-$	
0.996	0.996	0.000	44	0.19(5)	-0.49(9)	$\frac{7}{2}^-$	$\frac{3}{2}^-$	
	0.882	0.124	53	-0.77(3)	-0.24(6)		$\frac{5}{2}^-$	1.9(1)
	0.578	0.418	3				$\frac{3}{2}^-$	
1.265	1.141	0.124	100	0.35(6)	-0.28(8)	$\frac{9}{2}^-$	$\frac{5}{2}^-$	
1.361	1.361	0.000	51	-0.02(16)	0.25(20)	$\frac{3}{2}^-, \frac{5}{2}^-$	$\frac{3}{2}^-$	0.29(17), -0.18(11)
	1.237	0.124	24				$\frac{5}{2}^-$	
	0.943	0.418	17				$\frac{3}{2}^-$	
	0.406	0.755	9				$\frac{5}{2}^-$	
1.402	1.402	0.000	69				$\frac{3}{2}^-$	
	1.278	0.124	17				$\frac{5}{2}^-$	
	0.984	0.418	12				$\frac{3}{2}^-$	
	0.647	0.755	2				$\frac{5}{2}^-$	
1.659	1.535	0.124	78	-0.39(13)	-0.98(21)	$\frac{5}{2}^-, \frac{7}{2}^-$	$\frac{5}{2}^-$	1.4(9)
	1.241	0.418	22				$\frac{3}{2}^-$	
2.002	1.247	0.755	66	0.30(11)	-0.58(16)	$\frac{9}{2}^-$	$\frac{5}{2}^-$	
	1.006	0.996	34	-0.77(11)	0.13(18)		$\frac{7}{2}^-$	0.4(4)
2.099	1.975	0.124	100				$\frac{5}{2}^-$	
2.270	1.274	0.996	95	-0.26(10)	-0.51(14)	$\frac{7}{2}^-, \frac{11}{2}^-$	$\frac{7}{2}^-$	-1.9(4)
	1.005	1.265	5				$\frac{9}{2}^-$	
2.400	1.404	0.996	100				$\frac{7}{2}^-$	
2.797	1.532	1.265	100	-0.26(12)	-0.47(18)	$\frac{9}{2}^-, \frac{13}{2}^-$	$\frac{9}{2}^-$	2(1)
3.337	0.937	2.400	100				$\frac{7}{2}^-$	
4.413	1.076	3.337	100				$\frac{9}{2}^-$	

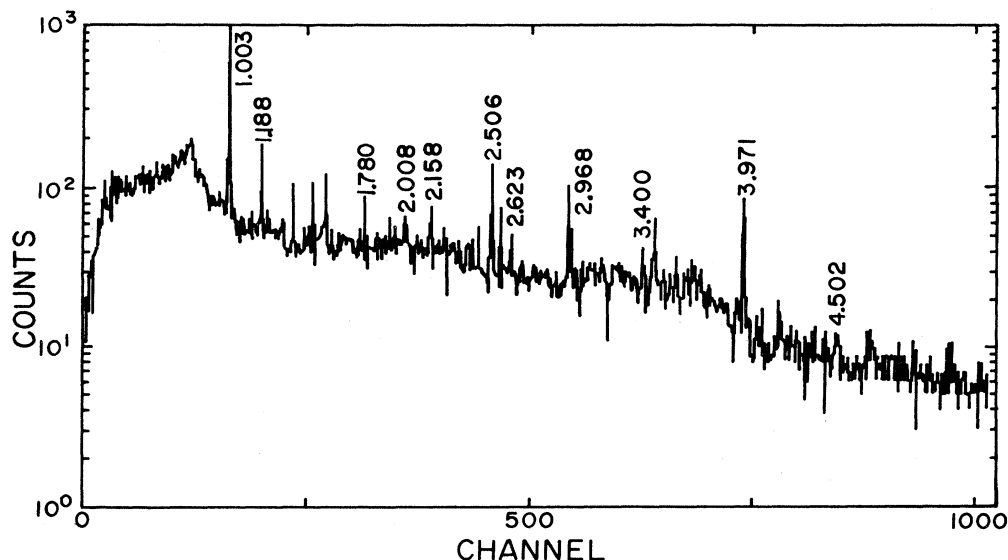


FIG. 7. $^{58}\text{Ni}(^3\text{He}, n\gamma)^{60}\text{Zn}$ neutron-gated spectrum at $E_{3\text{He}} = 12$ MeV.

found in the $^{40}\text{Ca}(^{23}\text{Na}, 2pn)^{60}\text{Cu}$ reaction. All the levels and transitions observed are summarized in Table IV and Fig. 11. The spins and parities come from Refs. 7 and 21.

IV. DISCUSSION

The level schemes resulting from this work and that of others may be compared with the shell-model calculations of Refs. 3 and 4. It is noteworthy that at the time the shell-model calculations were made little was known of the excited states of ^{60}Zn and nothing of ^{61}Zn . The 66 parameters of the adjusted surface delta interaction

(ASDI) were fitted to 101 levels of Ni and Cu isotopes with $57 \leq A \leq 66$ in Ref. 3 and consequently used to calculate levels of $^{57-67}\text{Ni}$ and $^{58-68}\text{Cu}$. Reference 4 used the same parameters to calculate levels of $^{60-68}\text{Zn}$. In ^{61}Zn , where more definite spin information is now available, the calculated and experimental levels are in accord up to 2.5 MeV. It seems likely that the heavy-ion experiments in which the higher levels were observed feed predominantly the yrast states, leaving many low-spin states undiscovered. There is a striking similarity between the level schemes of $^{60,61}\text{Zn}$ and $^{56,57}\text{Fe}$ ($N = 30, 31$, $Z = 28 \pm 2$).

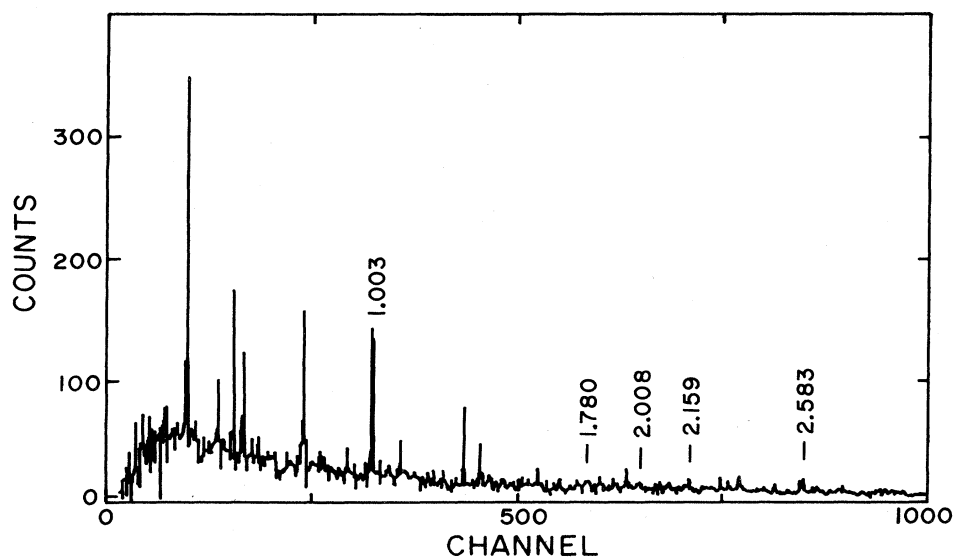
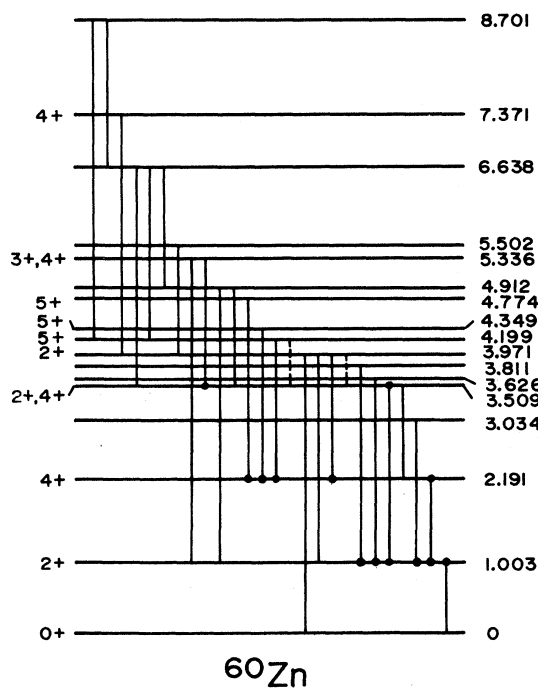


FIG. 8. $^{58}\text{Ni}(^3\text{He}, n\gamma\gamma)^{60}\text{Zn}$ neutron-gated coincidence spectrum at $E_{3\text{He}} = 12$ MeV. Gate: 1.189 MeV. The strong impurity lines are in ^{59}Ni (0.339, 0.547, 0.759, 1.342 MeV) and ^{60}Cu (0.339, 0.454, 1.399 MeV).

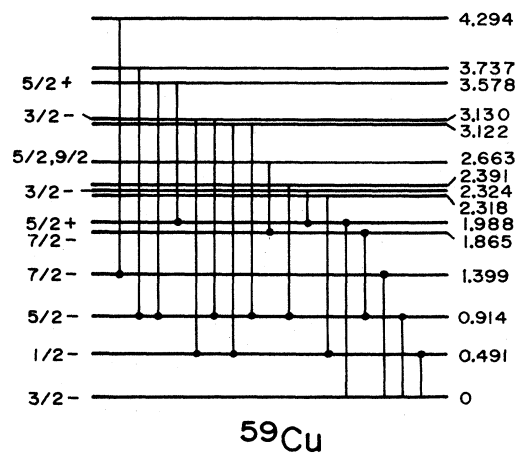
TABLE II. Levels and transitions in ^{60}Zn .

E_i	E_γ (MeV)	E_f	Branching ratio (%)	A_2	A_4	J_i^π	J_f^π	δ
1.003	1.003	0.000	100	0.49(2)	-0.09(2)	2^+	0^+	
2.191	1.188	1.003	100	0.50(2)	-0.26(3)	4^+	2^+	
3.034	2.031	1.003	100				2^+	
3.509	2.506	1.003	88	0.31(5)	-0.27(5)	$2^+, 4^+$	2^+	+3(1)
	1.318	2.191	12				4^+	
3.626	2.623	1.003	100				2^+	
3.811	2.808	1.003	100				2^+	
3.971	3.971	0.000	70	0.02(9)	-0.37(17)	2^+	0^+	
	2.968	1.003	10				2^+	
	1.780	2.191	14				4^+	
	0.462	3.509	6				$2^+, 4^+$	
4.199	2.008	2.191	67	0.43(17)	0.71(36)	5^+	4^+	-4(2)
	0.690	3.509	33				$2^+, 4^+$	
4.349	2.158	2.191	100	0.47(9)	0.36(12)	5^+	4^+	-3.5(5)
4.774	2.583	2.191	100	0.21(19)	0.44(23)	5^+	4^+	< -4.5
4.912	3.909	1.003	72				2^+	
	1.403	3.509	28				$2^+, 4^+$	
5.336	4.333	1.003	35				2^+	
	1.827	3.509	65	0.52(7)	0.14(12)	$3^+, 4^+$ or 3^+	4^+	+1.0(5), 0.0(2) +0.5(1)
							2^+	
5.502	1.531	3.971	100				2^+	
6.638	3.129	3.509	34				$2^+, 4^+$	
	2.439	4.199	47				5^+	
	1.726	4.912	19					
7.371	3.400	3.971	100	0.53(8)	-0.85(11)	4^+	2^+	
8.701	4.502	4.199	30				5^+	
	2.063	6.638	70					

FIG. 9. Proposed level scheme for ^{60}Zn .

A. ^{61}Zn

For the most part, these γ -ray results for ^{61}Zn agree with those of Smith *et al.*¹⁷ An exception is their proposal that the 2.002 MeV level is a $\frac{3}{2}^+$ state. The upper lifetime limit and strong decay to the $\frac{5}{2}^-$ 0.755 MeV level

FIG. 10. Levels of ^{59}Cu , showing the coincidence relations found.

make this seem unlikely. It is perhaps significant that the 1.006 MeV transition to the $\frac{7}{2}^-$ state on which the parity measurement of Ref. 17 rests was, in this work, contaminated by the 1.005 MeV transition higher in ^{61}Zn . This leaves as the most likely candidate for the $\frac{9}{2}^+$ state the 2.797 MeV level, but no parity determination has yet been made. If this is indeed the $\frac{9}{2}^+$ state, the decrease in excitation energy of the $g_{9/2}$ level with increasing A through the odd Zn isotopes would be quite smooth. The model calculation of Ref. 4 indicates that negative-parity levels of spin $\frac{9}{2}$ and $\frac{13}{2}$ are expected at this excitation energy as well.

The $^{40}\text{Ca}(^{24}\text{Mg}, 2pn)^{61}\text{Zn}$ reaction gives a further level at 4.413 MeV. Its decay, via two transitions to the $\frac{11}{2}^-$ state at 2.400 MeV suggests a spin of at least $\frac{15}{2}$. Three particle groups seen in the (α, n) reaction suggest further levels at 1.802, 2.357, and 2.484 MeV, but these have not been confirmed in any of the γ -ray or cluster transfer ex-

TABLE III. Levels and transitions in ^{59}Cu .

E_x	E_γ (MeV)	
2.318(1)	1.827(1)	a
2.324(1)	0.337(1)	b
2.391(1)	1.477(1)	b
2.663(1)	0.798(1)	a
3.122(1)	2.631(1)	c
	2.207(1)	c
3.130(1)	2.638(1)	a
	2.214(2)	a
3.580(1)	2.666(1)	a
	1.592(1)	a
3.737(2)	2.823(2)	c
4.294(2)	2.895(2)	c

^aLevel and γ seen in (p, γ) .

^bLevel seen in (p, γ) .

^cNew level, new γ .

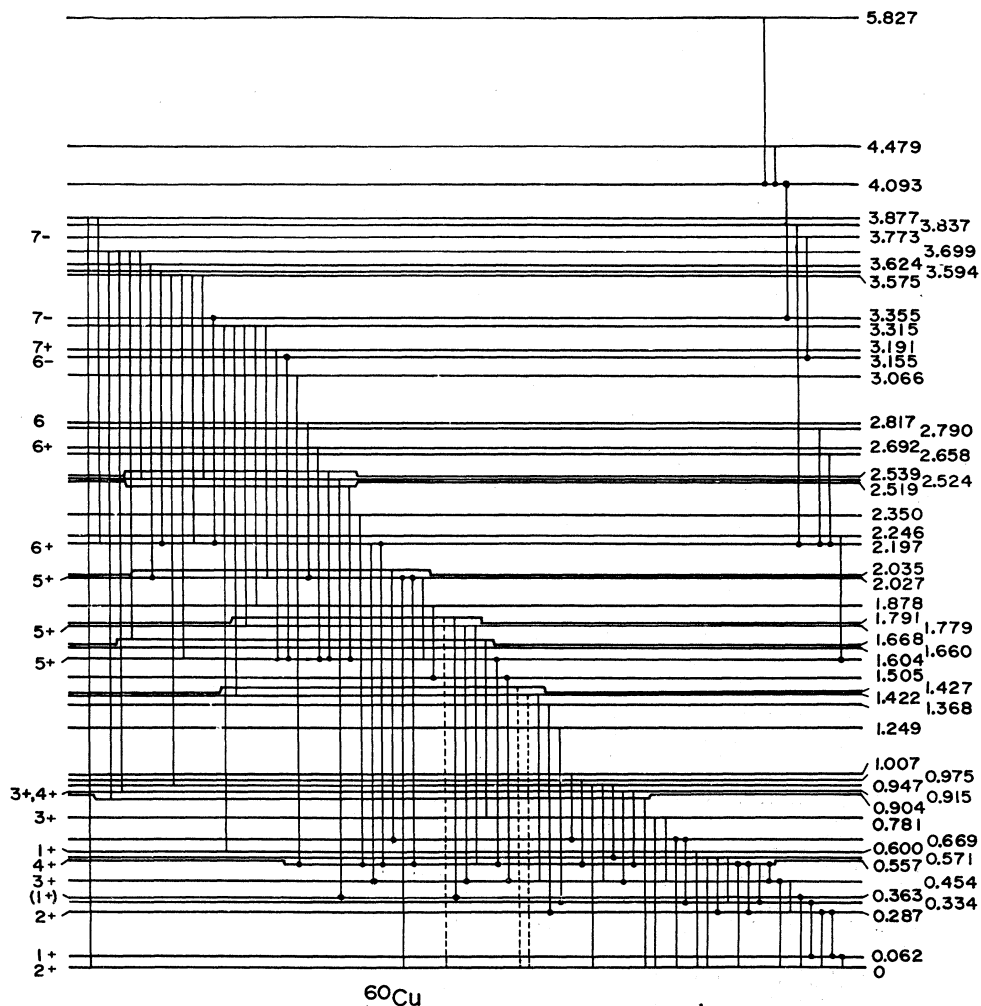
FIG. 11. Proposed level scheme for ^{60}Cu .

TABLE IV. Excited states observed in ^{60}Cu .

E_x (MeV)	$(^3\text{He}, p\gamma)^a$	$(HI, X\gamma)^a$	$(\alpha, np\gamma)^b$	$(p, n\gamma)$ and β decay ^c	$(^3\text{He}, t)$ and $(^3\text{He}, p)^c$
0.062	×	×	×	×	×
0.287	×	×	×	×	×
0.334	×	×		×	×
0.363	×	×		×	×
0.454	×	×	×	×	×
0.557	×	×	×		×
0.571	×				
0.600	×				×
0.669	×	×		×	×
0.781	×		×		×
0.904	×				
0.915	×	×	×		×
0.947	×			×	
0.975	×				
1.007	×	×			
1.249	×				
1.368	×				×
1.422	×	×	×		×
1.427	×				
1.505	×				×
1.604	×	×	×		
1.660		×			×
1.668	×				×
1.779	×		×		×
1.791	×				
1.878	×				
2.027	×	×	×		
2.035	×				
2.197	×	×	×		
2.246		×			×
2.350	×		×		×
2.519	×				
2.524	×				×
2.539	×				×
2.658		×			×
2.692	×		×		×
2.790		×			×
2.817	×		×		×
3.066	×		×		×
3.155	×	×	×		×
3.191	×		×		
3.315	×				×
3.355	×	×	×		×
3.594	×				×
3.624	×				
3.699	×				×
3.773		×	×		
3.837		×			
3.877	×				
4.093		×			×
4.479		×			
5.824		×			

^aPresent work.^bReference 21.^cReference 7.

periments.⁷ Of the twelve levels reported above 2.5 MeV in the cluster transfer experiments, only three, at 2.520, 2.979, and 3.337 MeV, were found in this work. The mass excess of $-56.369(8)$ MeV is in good agreement with the value $-56.352(20)$ found by Woods *et al.*¹⁴ from the $^{58}\text{Ni}(^6\text{Li},t)^{61}\text{Zn}$ reaction.

B. ^{60}Zn

The ^{60}Zn results confirm and extend the earlier ($^3\text{He},n\gamma$) work of Kamermans *et al.*⁸ All the levels observed in the ($^3\text{He},n$) experiments⁷ were found in this work, with the exception of the 5.200 MeV state.

Among the states found in the heavy-ion two-proton transfer reactions are a number of proposed analogs.¹² The 4.88 MeV 2^+ state seen in ($^{16}\text{O},^{14}\text{C}$) and suggested as the analog of the ^{60}Cu ground state^{7,12} may be the level observed here at 4.912 MeV, though no clear spin assignment is possible from the present results. Two $T=2$ states have been proposed, at 7.38 and 8.73 MeV, as analogs of the ^{60}Ni ground and first excited states. If the former is in fact the level found at 7.371 MeV in this work, the spin assignment of 0^+ is inconsistent with the large anisotropy of its 3.399 MeV γ decay. In this work, no spin assignment was possible for the 8.701 MeV level which may be the 2^+ analog. A number of states above 4 MeV have been identified¹³ as members of two-proton or two-neutron configurations involving $g_{9/2}$ nucleons. Few of the levels found in this study are consistent with these configurations, but this is hardly surprising in view of the undoubtedly high level density and the low angular momentum of the ($^3\text{He},n$) reaction.

A further spin assignment inconsistency between this work and the earlier studies is that at 3.509 MeV. The large A_4 coefficient in the angular distribution of the 2.506 MeV decay is difficult to reconcile with a $3^- \rightarrow 2^+$ interpretation. However, the lower resolution of the particle work makes positive identification of those levels with these difficult.

The shell-model calculations of Ref. 4 provide more levels between 3 and 5 MeV than have been observed in any of the experiments. The three 5^+ levels between 4 and 5 MeV are not predicted at such a low energy. This may be a peculiarity of the δ -function force used in the model calculation.

C. ^{59}Cu

Most of the ^{59}Cu levels found in this work are already summarized in Ref. 18. The presence of the 2.391 MeV level, suspected in (p,γ) singles work,^{19,20} is confirmed. The 3.122 MeV level has not previously been observed. The 3.737 and 4.294 MeV levels may be the same as the previously reported 3.742 and 4.301 MeV states, although the decays observed do not agree closely. It is

likely that the second $\frac{7}{2}^-$ level at low energy is a $f_{7/2}$ hole state, similar to those seen in other odd Cu nuclei and in the $N=29$ isotones.

D. ^{60}Cu

This study has located most of the known levels of ^{60}Cu up to 3.8 MeV and a number of (presumably) high-spin states beyond. Table IV presents a summary of the comparison of these results with those of previous studies. The most exhaustive of these is that of Chan *et al.*²¹ using the $^{58}\text{Ni}(\alpha,np\gamma)^{60}\text{Cu}$ reaction. All of their levels and transitions are confirmed in this work. The 0.947 MeV level was previously seen weakly in the decay of ^{60}Zn .²² This and several other observed levels likely correspond to those found in ($^3\text{He},p$) and ($^3\text{He},t$) measurements.²³⁻²⁵ The eight further transitions found in the $^{40}\text{Ca}(^{23}\text{Na},2pn\gamma)^{60}\text{Cu}$ reaction extend both the positive- and negative-parity high-spin levels established in Ref. 21.

The 0^+ level reported at 2.536 MeV from ($^3\text{He},p\gamma$) (Ref. 23) and interpreted as the analog of the ^{60}Ni ground state may be one of the three levels found here near that energy. Two of them, however, at 2.519 and 2.539 MeV, decay to the 5^+ 1.604 MeV level and are therefore excluded as 0^+ candidates. The only observed decay of the central level at 2.524 MeV was to the 0.363 MeV state (1^+). The 3.877 MeV level is unlikely to be the 3.874 MeV state found in ($^3\text{He},p$) and ($^3\text{He},t$) with a tentative $L=2$ transfer and proposed as the analog of the 1.333 MeV first excited state of ^{60}Ni .^{24,25} From its decay to both the 2^+ ground state and the 6^+ 2.197 MeV level, the 3.877-MeV state is undoubtedly 4^+ .

V. CONCLUSIONS

The spectroscopy of light Cu and Zn isotopes reported here confirms and extends earlier gamma-ray and particle studies. A number of significant discrepancies remain to be resolved. In particular, the identification of the $g_{9/2}$ state in ^{61}Zn is uncertain, as is that of the $(J^\pi, T)=(0^+, 2)$ level of ^{60}Zn . A potential 0^+ analog in ^{60}Cu at 2.524 MeV exists but the level observed in this work at 3.877 MeV is not the proposed 2^+ analog state. It is noteworthy that the experimental level schemes, now fairly well developed, are in good accord with the shell-model calculations, which long preceded them.

ACKNOWLEDGMENTS

The authors are grateful to the tandem operations staff for their help. The loan of the Seforad neutron detector by W. V. Prestwich is much appreciated. The work was supported by grants from the Natural Sciences and Engineering Research Council of Canada.

*Present address: Department of Physics, University of Saskatchewan, Saskatoon, Saskatchewan, Canada and TRIUMF, 4004 Wesbrook Mall, Vancouver, British Columbia, Canada.

†Present address: Atomic Energy of Canada Ltd., Chalk River Nuclear Laboratories, Chalk River, Ontario, Canada.

¹M. L. Rustgi, Phys. Rev. C **4**, 854 (1971).

²A. Jaffrin, Nucl. Phys. A **196**, 577 (1972).

- ³J. E. Koops and P. W. M. Glaudemans, *Z. Phys. A* **280**, 181 (1977).
- ⁴J. F. A. Van Hienen, W. Chung, and B. H. Wildenthal, *Nucl. Phys. A* **269**, 159 (1976); Michigan State University Cyclotron Laboratory Report No. 235, 1977.
- ⁵V. K. Thankappan and W. W. True, *Phys. Rev.* **137**, B793 (1965).
- ⁶S. S. M. Wong, *Nucl. Phys. A* **159**, 235 (1970).
- ⁷P. Andersson, L. P. Ekström, and J. Lyttkens, *Nucl. Data Sheets* **48**, 251 (1986).
- ⁸R. Kamermans, H. W. Jongsma, J. van der Spek, and H. Verheul, *Phys. Rev. C* **10**, 620 (1974).
- ⁹M. B. Greenfield and C. R. Bingham, *Phys. Rev. C* **6**, 1756 (1972).
- ¹⁰D. Evers, W. Assmann, K. Rudolph, and S. J. Skorka, *Nucl. Phys. A* **230**, 109 (1974).
- ¹¹D. J. Weber, G. M. Crawley, W. Benenson, E. Kashy, and H. Nann, *Nucl. Phys. A* **313**, 385 (1979).
- ¹²Y. Ōkuma, T. Motobayashi, K. Takimoto, S. Shimoura, M. Fukada, T. Suehiro, and T. Yanabu, *Research Center for Nuclear Physics Annual Report*, 1984, p. 104.
- ¹³A. Boucenna, L. Kraus, I. Linck, J. C. Sens, and Tsan Ung Chan, *Institut National de Physique Nucléaire et de Physique des Particules Annual Report*, 1985 (submitted to *Phys. Rev. C*).
- ¹⁴C. W. Woods, N. Stein, and J. W. Sunier, *Phys. Rev. C* **17**, 66 (1978).
- ¹⁵L. P. Ekström and J. Lyttkens, *Nucl. Data Sheets* **38**, 463 (1983).
- ¹⁶D. G. Sarantites, J. H. Baker, N. H. Lu, E. J. Hoffman, and D. M. Van Patter, *Phys. Rev. C* **8**, 629 (1973).
- ¹⁷P. J. Smith, L. P. Ekström, F. Kearns, P. J. Twin, and N. J. Ward, *J. Phys. G* **8**, 281 (1982).
- ¹⁸P. Andersson, L. P. Ekström, and J. Lyttkens, *Nucl. Data Sheets* **39**, 641 (1983).
- ¹⁹H. V. Klapdor, M. Schrader, G. Bergdolt, and A. M. Bergdolt, *Nucl. Phys. A* **245**, 133 (1975).
- ²⁰G. U. Din, J. A. Cameron, V. P. Janzen, and R. B. Schubank, *Phys. Rev. C* **31**, 800 (1985).
- ²¹Tsan Ung Chan, M. Agard, J. F. Bruandet, B. Chambon, A. Dauchy, D. Drain, A. Giorni, F. Glasser, and C. Morand, *Phys. Rev. C* **26**, 429 (1982).
- ²²G. H. Dulfer, T. J. Ketel, A. W. B. Kalshoven, and H. Verheul, *Z. Phys.* **251**, 416 (1972).
- ²³D. P. Balamuth and E. G. Adelberger, *Phys. Rev. C* **16**, 928 (1977).
- ²⁴H. J. Young and J. Rapaport, *Phys. Lett.* **26B**, 143 (1968).
- ²⁵H. Rudolph and R. L. McGrath, *Phys. Rev. C* **8**, 247 (1973).
- ²⁶J. E. McFee, Ph.D. thesis, McMaster University, 1977.
- ²⁷H. J. Rose and D. M. Brink, *Rev. Mod. Phys.* **39**, 306 (1967).
- ²⁸A. N. James, P. J. Twin, and P. A. Butler, *Nucl. Instrum. Methods* **115**, 105 (1974).
- ²⁹P. M. Endt, *At. Data Nucl. Data Tables* **23**, 547 (1979).